# SEMM-2: A Modeling System for Single Event Upset Analysis

Henry H. K. Tang, *Member, IEEE,* and Ethan H. Cannon

***Abstract*—We describe SEMM-2, a new simulation system for the analysis of radiation-induced single event upsets which builds on the initial SEMM tool. Developed for the current and future CMOS technologies, SEMM-2 improves the generation of radiation events. The atomic databases which describe ion energy loss with transport through device materials are generalized. Enhancements of the nuclear collision event generation include more accurate and efficient methods for generating elastic events and more thorough treatment of inelastic processes. We present illustrative simulations where more accurately accounting for the metallization layers significantly impacts the simulated single event failure rate.**

***Index Terms*—Alpha particle-, proton-, neutron-, high-energy hadron-, cosmic ray-, and heavy ion-induced radiation in microelectronics, CMOS technology stability and reliability, particle-induced soft errors, single event upsets, radiation effects, radiation effects modeling methodology and simulation tools.**

## I. Introduction

IN ORDER to study the critical technology issues raised by single event upsets (SEUs) induced by alpha particles in packaging materials and by background terrestrial cosmic neutrons, a comprehensive SEU simulation system, the soft error Monte Carlo model (SEMM), was developed in 1986. For many years it has been the key SEU analysis tool for IBM bipolar product developments. In this paper, this first SEU model will be referred to as SEMM-1. The basic physics and simulation techniques incorporated in SEMM-1 have been documented in a series of publications [1]–[6].

Recent advances in semiconductor technology—including the continued progress of scaling, with the accompanying reduction both in circuit critical charge (Qcrit) and device sizes, and the introduction of new materials, such as boron phosphate silicate glass (BPSG) and hydrogen-containing low-$k$ dielectric materials—have spawned a renewed interest in SEU studies and a realization of the need to go beyond the original SEMM-1 model. In this paper, we report on our latest progress in SEU modeling with a new program, SEMM-2, which has been developed for the current and future CMOS technologies. Though SEMM-2 adopts many of the modeling techniques developed in the original SEMM-1 program, it has added a number of important features to address new SEU issues. The most significant advances include improved and efficient cosmic ray collision simulations that incorporate both elastic and inelastic events and capabilities to analyze arbitrary new materials, more careful tracking of radiation particles through metallization (e.g., W, Al, Ta, Cu), and the ability to include the cosmic ray spectrum in parametrized form to estimate the terrestrial cosmic-ray-induced SEU rate.

Manuscript received July 20, 2004.

H. H. K. Tang is with IBM T. J. Watson Research Center, Yorktown Heights, NY 10598 USA (e-mail: hktang@us.ibm.com).

E. H. Cannon is with IBM Systems and Technology Group, Essex Junction, VT 05452 USA.

Digital Object Identifier 10.1109/TNS.2004.839507

## II. Modern SEU Concerns and SEMM-2 Developments

The developments of SEMM-2 have been driven by SEU issues of the current CMOS technologies. Here we summarize some of the most important motivations.

1) The typical critical charge of a bipolar chip analyzed by SEMM-1 was of the order of 100 fC. In contrast, the critical charge of modern CMOS technologies is only a few fCs. With such significant decrease in Qcrit, the details of the interactions between radiation particles and active silicon become important. Hence it is imperative to simulate accurately the transport of charge particles (i.e., alpha particles from IC materials, or the secondary nuclear fragments from neutron spallation reactions) through device/circuit materials.
2) With their reduced Qcrit values, new technologies exhibit an increased sensitivity to neutrons below 50 MeV [7]. This demands close examination of the adequacy of the nuclear reaction models that provide the essential inputs for SEU simulations (e.g., nuclear cross sections, and the generation of nuclear collision events). Also, below 50 MeV, the terrestrial neutron flux rises rapidly with decreasing neutron energy. Hence new and accurate cosmic neutron flux models are essential inputs for the simulations of cosmic-ray-induced SEUs.
3) Technology scaling leads to decreased feature sizes in each generation, as well as lower Qcrit values. Predicting the combined results of these competing factors is increasingly important for future chip designs. Decreasing per bit soft fail rates with increasing chip-level soft error rates haven been reported in [7]–[9].
4) With the introduction of new materials and the increased SEU sensitivity of lower Qcrit devices, cosmic ray interactions with the new materials must be considered.
5) Thermal neutrons have been observed to cause soft fails in some recent technologies [7], [8]. The thermal neutrons are produced by MeV neutrons slowed down by collisions with materials near the device. As such, practical parametric models of terrestrial neutron flux that cover a wide range of neutron energies from GeV down to MeV is a very useful feature in new SEU simulation tools [10].

0018-9499/04$20.00 © 2004 IEEE

Authorized licensed use limited to: Intel Corporation via the Intel Library. Downloaded on February 27, 2009 at 14:59 from IEEE Xplore. Restrictions apply.

6) For bulk technologies, it has been well established that the major charge collection mechanism is due to field-assisted funneling. For new technologies like silicon-on-insulator (SOI), charge collection mechanisms other than funneling are at work [11].

New SEU models are needed to address these charge transport and circuit issues at a fundamental level.

## III. Major Features and Enhancements in SEMM-2

Accurate simulations of SEUs require several advanced computational tools. Modeling high-energy neutron or proton collisions with the nuclei in the semiconductor chip requires state-of-the-art nuclear reaction models. Atomic models are required to describe ionization from a charged particle's motion through the circuit/device materials. Sophisticated device simulators are essential to follow the rapid generation of a large quantity of free charge, which can drastically alter the electrostatic potentials, as in the case of funneling in bulk devices, and can modify device behavior, as in the case of parasitic bipolar gain in SOI devices. Estimating the SEU rate of a particular circuit mandates considering the circuit response to a variety of radiation particle trajectories, from direct hits to the sensitive node, to near misses at various angles to the substrate normal. Simulation time precludes the ideal detailed study of a representative sample of radiation events with state-of-the-art device simulators. The approach in SEMM-1, followed by SEMM-2, is to simplify the charge collection component for the sake of computing speed, and to perform a Monte Carlo sampling of radiation events. With this approach, it is possible to estimate the appropriate ensemble of radiation particle trajectories. Given the focus on sampling the radiation events, in developing SEMM-2 we concentrate our efforts on radiation event generation. While this approach does not resolve all of the issues raised in the previous section, it ameliorates the critical portion of the SEU simulation process and specifically addresses problems 1) through 5).

The flow chart in Fig. 1 outlines the major components of SEMM-2. In general, there are three major steps involved in SEU simulations: 1) the generation of a radiation event; 2) charge transport and collection for that event; and 3) postprocessing to determine whether the radiation event causes an upset. The essential inputs to the radiation event generation include atomic databases and nuclear databases. The atomic databases consist of tables of linear energy transfer (LET) and energy-range relations of ions in various important materials such as silicon, copper, and silicon dioxide. These tables are needed for calculations of particle transport and energy deposition in the device/circuit materials. The data in these tables are accessed by fast and accurate interpolation algorithms. The nuclear databases are required for the simulations of proton, neutron, and pion events. They consist of elastic and inelastic (reaction) cross sections of hadron-nucleus reactions from a few MeV up to about 1 GeV. These nuclear databases also consist of reaction history files that contain full kinematic information of the secondary particles produced in high-energy inelastic hadron-nucleus collisions. The elastic collision events require elastic cross sections which are taken from compiled data or

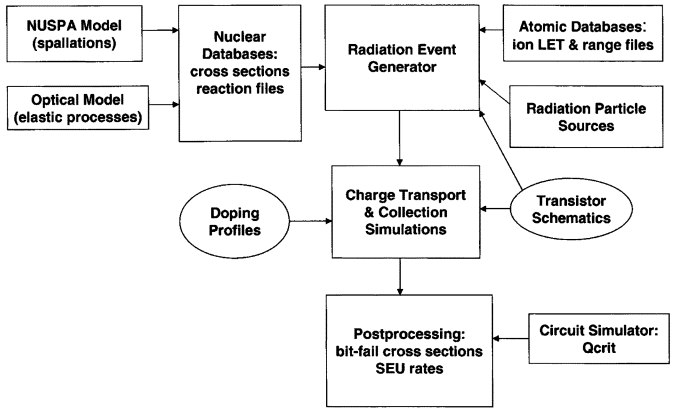


Fig. 1. Flow chart of SEMM-2 showing the major components and their inter-relations.

generated by standard nuclear optical models. The inelastic collision events require both inelastic cross section tables as well as reaction files. These data are generated by a state-of-the-art nuclear spallation reaction model NUSPA developed by the first author for IBM's SEU research program [5], [6].

The NUSPA model is a critical part of this SEU modeling methodology. Over the years it has been well tested by a large quantity of measured nuclear data [5], [6], [12]. The NUSPA model is based on a framework of intranuclear cascade processes and compound nucleus reactions; it simulates proton–, neutron–, and pion–nucleus reactions from MeV to several GeVs. Its theoretical foundation has been discussed in [5] and [6].

The simplified charge collection in SEMM-2 does not include the full circuit response to a radiation event. So the postprocessing requires appropriate Qcrit values from circuit simulators as inputs to determine whether the current pulse from a given radiation event is large enough to induce a soft error. Fig. 2 shows a typical layout geometry for SEMM-2. The event generation routine determines the ionization radiation trajectory. In the case of an alpha particle hit, the event generator provides the alpha particle birth location and trajectory through the packaging materials. In the case of a cosmic ray event, the event generator provides the secondary particles produced from the cosmic-ray–nucleus reaction, the birth location of these secondary particles, and their trajectories. During step 2), charge is generated in the active silicon layer; charge collection by the built-in electric field of a reverse-biased junction occurs by 3-D drift-diffusion or funneling within the funneling channel using techniques from SEMM-1 [4].

SEMM-2 has several important improvements over SEMM-1 in the radiation event generation step. For instance, SEMM-2 can handle any number of metallization and dielectric layers and materials. The transport of each charged particle (proton, heavy ion, or charged pion) through material stacks is followed in detail. The calculations of particle transport and energy deposition in sensitive volumes are performed with accurate lookup algorithms applied to a large atomic database of particle ranges and LETs in a number of technologically important materials including, for example, novel low-$k$ dielectrics and copper metallization.

Authorized licensed use limited to: Intel Corporation via the Intel Library. Downloaded on February 27, 2009 at 14:59 from IEEE Xplore. Restrictions apply.

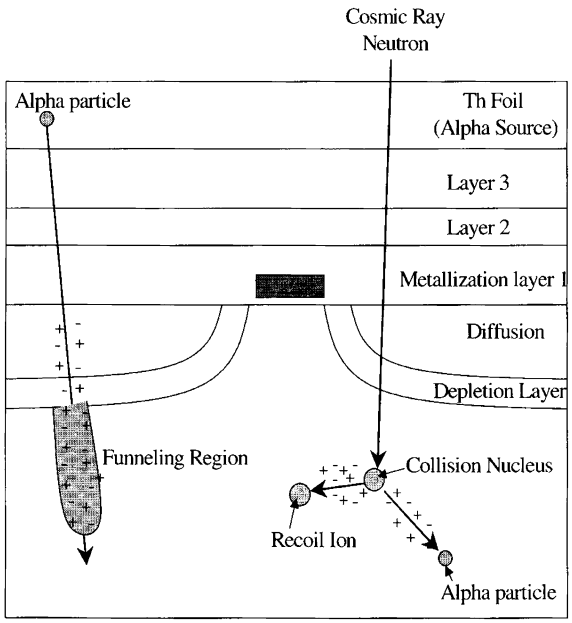


Fig. 2. Geometry of a typical transistor represented in SEMM-2, showing the metallization levels, diffusion regions and depletion regions. Examples of an alpha particle event (with funneling) and a cosmic ray neutron event (with spallation reaction) are also shown.

In the case of irradiation by high-energy protons, neutrons, and pions, the nuclear events—which can be elastic or inelastic scattering (as in the case of spallation reactions)—are generated by Monte Carlo sampling techniques, with the help of cross sections computed by the NUSPA code and nuclear optical models. The multiplicity of secondary fragments from high-energy reactions is readily handled by the NUSPA code which provides exclusive reaction channels as outputs [5], [6]. This important feature of NUSPA provides SEMM-2 the capability of analyzing multiple-bit fails.

The next several subsections detail how SEMM-2 augments the radiation event generation step of the SEU simulation methodology.

### A. Enhancements of Nuclear Databases (Inelastic Processes)

SEMM-1 deals primarily with silicon, using databases of proton-Si and neutron-Si reactions as inputs for SEU simulations. The inelastic reaction databases are simulated by the nuclear spallation reaction model NUSPA [5], [6]. Each database consists of a number of reaction history files for a particular incident particle energy, which contain the full kinematic information of the secondary particles (particle type, energy and direction of velocity vector) in an event by event basis. The outputs from the NUSPA code consist of secondary protons, neutrons, deuteron, triton, He, Li, etc., and heavy residual recoil nuclei. Secondary pions can be produced when the kinetic energy of the incident proton or neutron exceeds 300 MeV. SEMM-1 was developed when typical Qcrit values were of the order of 100 fC and low LET protons, deuterons, tritons and charged pions were unable to cause SEUs; to save computer processing time and to trim the database size, these particles were filtered from SEMM-1 databases. Neutrons were also filtered away since they do not cause direct ionization and nuclear reactions they might initiate are high-order effects that could be neglected.

In SEMM-2 we have reconstructed these Si databases with the latest version of NUSPA, including all charged secondary fragments produced in the reactions since SEMM-2 is geared toward the extremely low Qcrit circuits in current and future CMOS technologies. An important motivation for SEMM-2 enhancements is to develop modeling capabilities for analysis of the SEU sensitivity in exploratory product designs which incorporate new materials like low-$k$ dielectrics. We have generated new databases for materials such as O, C, Cu, etc.; we have also generated a new database of proton-proton and proton-neutron cross sections (0–2 GeV). Whereas the SEU cross sections for the bipolar chips were negligible at incident proton/neutron energies below 50 MeV, for recent technologies this threshold energy has gone down considerably. The current history files in SEMM-2 cover the energy range from 20 MeV to 1 GeV.

### B. Enhancements of Nuclear Databases (Elastic Processes)

SEMM-1 stores information for elastic reactions in history files, as for inelastic reactions. For SEMM-2, we have developed an efficient algorithm to generate elastic events, which is superior to the large and computationally inefficient history files used in SEMM-1. We generate short tables of scattering probabilities computed from a nuclear optical model; these tables are stored as part of the nuclear database. In a given application, Monte Carlo techniques [13] are used to generate an ensemble of proton or neutron scattering angles. Then the recoil energy corresponding to each value of scattering angle is computed analytically. Such calculations are fast—an ensemble of a million elastic events can be generated in a few CPU seconds on a workstation. In contrast, to simulate an ensemble of inelastic events (using NUSPA code) with the same size, depending on the target nucleus mass number and the incident energy, it can take several CPU hours on the same machine. In short, in SEMM-2, elastic events are simulated in each proton or neutron run, and no history file is required to store these events. Simulations of inelastic events are much more complex and hence much more CPU consuming, thus the inelastic events are stored in large files just as in SEMM-1.

For a detailed analysis of the relative importance of elastic and inelastic scattering events, see [5]. Here we outline the key points to illustrate the importance of elastic scattering events in current technologies. The elastic cross section (differential cross section integrated over all angles) at high energies ($>$100 MeV) is of the same order of magnitude as the inelastic cross section; but at lower energies, say, below 50 MeV, the elastic cross section is larger than the inelastic cross section and rises with decreasing energy. The differential elastic cross section is forward-peaked (see Fig. 4(a) of [5]); in other words, in most elastic events the proton or neutron (in the laboratory frame) goes into a small scattering angle, and large-angle scatterings (which transfer more energy to the recoil nucleus) are very rare events. Fig. 4(b) of [5] shows the recoil energy of a Si target plotted against the scattering angle of a colliding proton for four reactions at 50, 100, 250, and 500 MeV. As a numerical example, an incident 100-MeV proton scattered into an angle of 7° is associated with a target recoil energy of

Authorized licensed use limited to: Intel Corporation via the Intel Library. Downloaded on February 27, 2009 at 14:59 from IEEE Xplore. Restrictions apply.

about 60 keV; this recoil energy, in turn, generates 2.67 fC of electrons and holes. Clearly for a circuit with Qcrit of 100 fC, this elastic event will not flip the state. However in modern circuits whose Qcrit values are below 10 fC, elastic events are important contributions to SEUs.

### C. Enhancements of Atomic Database

In order to track the transport of a radiation particle from the point where it is created to the point it reaches the active silicon, accurate and efficient calculation of energy deposition is essential; this requires the LET and energy-range relations of a variety of ions in several materials. SEMM-1 codes the energy-range tables of proton, alpha and some representative heavy ions in a small number of materials in various subroutines. Such a computational setup for LET, however, does not give the high accuracy that is required by the new devices we study. Also, from a programming standpoint, this setup does not have the flexibility that allows us to add energy-range data for new materials without a lot of programming effort.

SEMM-2 employs a new atomic database: Tables of the LET and energy-range relation for ions in a number of important materials (such as Si, $SiO_2$, Al, Cu, low-$k$ materials, Pb, etc.) are compiled using the SRIM simulation code [14]. A family of general-purpose interpolation subroutines facilitates the use of the database; for example, the LET of an ion in a given material at an arbitrary energy is computed by table lookup and interpolation. The energy grids in these tables are allowed to be arbitrarily distributed, and the interpolation subroutines offer the options of using linear-linear, linear-log, log-linear, and log-log interpolation algorithms. The database has a simple format, and adding new data files for future updates would involve very minimal work.

### D. New Radiation Event Generator

In SEMM-2, major efforts have been made to write a new radiation event generator. These efforts are necessary because SEMM-1 is capable of treating only very simplistic geometries of the metallization layers. The intent of the new radiation event generator is to provide a basic module which will easily accommodate new simulation options. In a typical layout geometry for SEMM-2, such as the one shown in Fig. 2, the event generation routine determines the ionization radiation trajectory, which can be from an alpha emitted from the packaging materials, or from a secondary charged fragment produced by the collision between a high-energy cosmic particle (neutron, proton, or pion) with a nucleus.

In an alpha particle event, the event generator provides the alpha particle birth location and trajectory through the packaging materials. The alpha is emitted from a finite source volume which can have one of a number of convex shapes such as sphere, cylinder or rectangular bar. The alpha can also come from a thin foil on the top of the metallization; this feature allows us to perform numerical simulations to compare with the thorium foil experiments often used to study alpha sensitivities. The positions and dimensions of these alpha source objects are initialized by the user. In a simulation, a random birth location of the alpha is first selected, and then a random emission direction is determined. The location of the exit point on the surface of the source volume is computed; the code, using the alpha energy-range data, determines whether the alpha will be absorbed in the volume, or it will have enough energy to reach the surface. In the former case, the simulation will start again with another alpha. In the latter case, the code will determine the energy left as the alpha reaches the surface point. At this stage, the transport of the alpha will be followed just like other charged particles produced by cosmic ray hits.

In a cosmic ray event, the event generator provides the secondary particles produced from the cosmic ray-nucleus reaction, the birth location of these secondary particles, and their trajectories. To illustrate the simulation strategy, we consider the example of a high-energy neutron coming from the top side of the back end materials as shown in Fig. 2. First, the nuclear collision point is constructed as follows. The code selects a random location as a starting point. Based on the angular distribution of the neutron, the neutron direction is determined by Monte Carlo sampling. From the initial location and the unit direction vector, the neutron path length through each metallization level is computed. The mean free path in each layer can be computed from the knowledge of the total nuclear cross section. For example, in the $i$th layer, the length of the mean free path is computed by the standard formula

$$\lambda_i = (\rho_i \sigma_{\mathrm{tot}\,i})^{-1}. \tag{1}$$

In (1), $\rho_i$ is the atomic number density of the material (number of atoms per unit volume), and $\sigma_{\mathrm{tot}\,i}$ is the total cross section of neutron-nucleus reaction. Here we assume that the layer consists of one atomic species; a generalization of (1) to the case of a composite material is obvious. From these mean free-path lengths, the collision point is determined by standard Monte Carlo sampling procedures. At the collision point, the code selects a collision event from the nuclear database. The nuclear collision point becomes the birth location of the secondary charged particles. Each particle will then be followed until one of the following possibilities happens: a) the particle hits the active silicon surface; b) the particle gets absorbed in the metallization materials because of lack of energy; or c) the particle leaves the system through the side boundaries. If the particle moves away from the active silicon surface, it is treated as if it is eventually absorbed in the system. In case a), the particle energy, hit location on the active silicon surface and direction of the velocity vector are stored for later analysis. In the cases b) and c), the code starts all over with another cosmic neutron.

### E. New Parametric Model of Terrestrial Neutron Flux

In order to compute the absolute SEU rate (FIT rate) of a circuit due to the cosmic neutrons at a location, it is essential that a realistic energy distribution of the neutrons enters the simulations. In SEMM-1, no realistic energy distribution is used.

Recently a new parametric model has been developed to compute the terrestrial neutron fluence rate spectrum (energy differential flux in units of incident neutron number/$cm^2$-s-MeV). This model is based on new and state-of-the-art neutron measurements covering an energy range from meV up to GeV range, and can be expressed in simple analytic form. Details of these

Authorized licensed use limited to: Intel Corporation via the Intel Library. Downloaded on February 27, 2009 at 14:59 from IEEE Xplore. Restrictions apply.

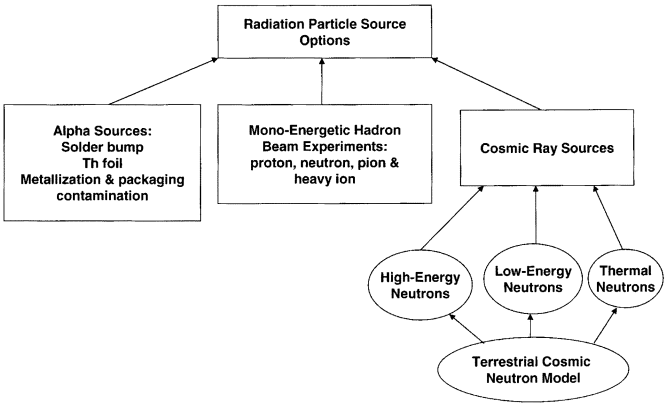


Fig. 3. SEMM-2 simulation options with a variety of particle sources.

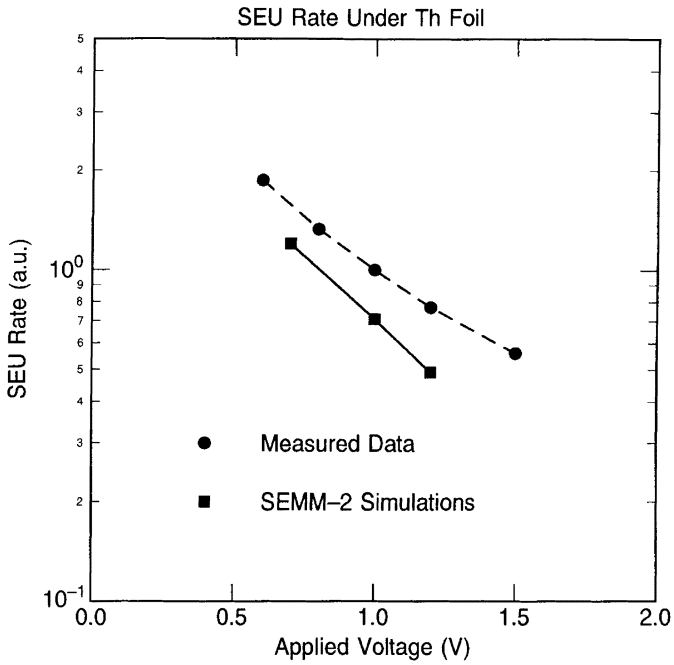


Fig. 4. SEU rate as function of applied voltage. The soft fails are caused by alphas emitted from a thorium foil in the back end. The curves show the measured data and simulations by SEMM-2.

measurements and the model are discussed in [10], and they will not be repeated here. It suffices to say that the model, being correlated with accurate data, has incorporated realistic dependence on altitude and geomagnetic effects. This model has been integrated as an option in SEMM-2.

*Remarks on Normalization:* It is emphasized that absolute calculations are done in SEMM-2 simulations. In calculating an SEU cross section, which is a fundamental parameter to characterize a circuit's SEU sensitivity, SEMM-2 does not require any adjustment or normalization relative to a reference circuit, or to some prior measurement data. SEMM-2 is a scheme that simulates actual experiments; this capability of calculating absolute SEU cross section implies that SEMM-2 results can be directly confronted with experimental measurements without any ambiguity.

## IV. Primary Options of SEMM-2 and Examples

Fig. 3 shows the primary options of radiation particle source in SEMM-2: 1) simulations of high-energy mono-energetic proton-, neutron-, and pion-beam experiments to generate proton-, neutron-, and pion-induced SEU cross sections of circuits; 2) simulations of mono-energetic heavy ion beam experiments to generate heavy ion-induced cross sections; 3) simulations of alpha sources from the metallization and packaging materials; and 4) simulations of SEUs from cosmic ray neutrons, including high-energy, low-energy, and thermal neutrons, using parametric terrestrial neutron flux models [10].

Here as illustrative examples we show some SEMM-2 simulations of a 6-T SRAM in IBM's 90-nm bulk CMOS technology; SEMM-2 can simulate other circuits, such as multiport SRAMs, latches, dominos, etc. Thorium foil and proton beam data were collected with an SRAM array on a test chip with no voltage regulator, so varying the applied voltage (VDD) changes the radiation sensitivity through Qcrit. The proton beam tests were conducted at the Northeast Proton Therapy Center, Boston, MA.

The first step in SEMM-2 simulations is to define a unit cell on a rectangular grid by specifying charge-collecting depletion layers, diffusions, N-well, and substrate regions, and areas of field oxide. The unit cell is translated and copied to form the chip; the simulation chip need not be the same size as the physical chip, as long as it is larger than all important physical features, e.g., solder bumps, to minimize edge effects. SEMM-2 uses vertical doping profiles in the charge transport and collection step; in addition, the funneling calculation in this step incorporates user-defined parameters describing the extent of the funneling region. The chip geometry and charge collection have been described in detail in references about SEMM-1 [4]. Funneling parameters are generally obtained by comparing current pulses from SEMM-2 simulations with current pulses from sophisticated device simulators, see, e.g., [15], while ensuring parameters are consistent with the doping profiles, and by modifying the parameters for future technologies based on process changes. We use the same funneling parameters for all simulations in a given technology since Monte Carlo simulations are used not only to understand accelerated test results (where we could adjust funneling parameters to optimize the fit with measurements), but also to predict the SEU for devices and sources not included in the accelerated testing regiment (where such funneling parameter optimization is not possible) [9].

*Example 1: Alphas From Thin Thorium Foil:* Fig. 4 shows alpha-induced soft fail rate of an SRAM in IBM's 90-nm bulk CMOS technology as a function of applied voltage. The alphas are emitted from a thorium source. Both the experimental and theoretical curves fall with increasing voltage at approximately the same rate, though the measured data are consistently higher than the simulation data by about 1.5 times. This level of agreement is quite acceptable to assess the SER sensitivity of a circuit in order to make informed decisions of chip-level SER mitigation needs.

*Example 2: Effects of Metallization on SEU:* To demonstrate the importance of correctly accounting for the composition of

Authorized licensed use limited to: Intel Corporation via the Intel Library. Downloaded on February 27, 2009 at 14:59 from IEEE Xplore. Restrictions apply.

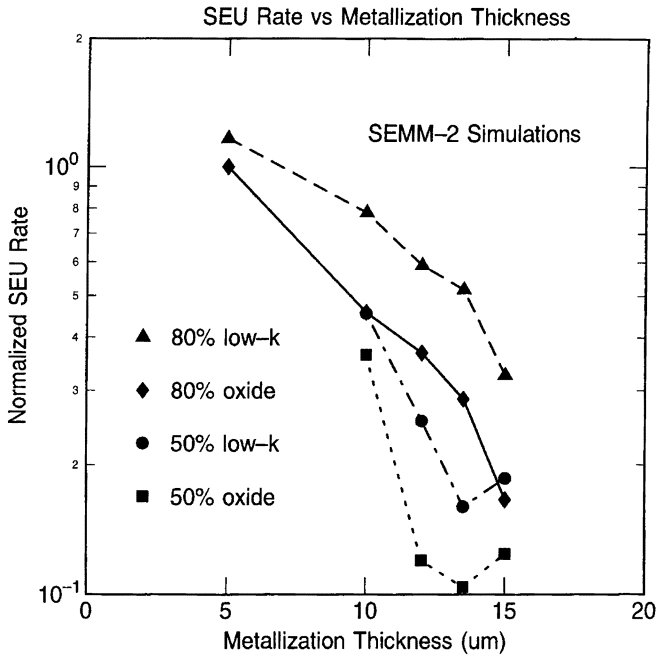


Fig. 5. SEU rate as function of metallization thickness. Effects of various combinations of oxide and low-$k$ material are analyzed by SEMM-2.

the metallization layers, we performed thorium foil simulations with different dielectric materials (oxide or a CVD low-$k$ dielectric) and different metallization thickness (total thickness from 5 to 15 $\mu$m). We represent the metallization as spatially uniform layers of dielectric and copper; to demonstrate the importance of metal wiring density, we conduct simulations where copper represents 20% or 50% of the total metallization thickness. The metallization thickness in ICs depends on the number of metallization levels. Fig. 5 presents the normalized fail rate at 1.2 V as a function of metallization thickness. Oxide has a higher LET because of its greater density, thus it attenuates alpha particles more efficiently and the fail rate is lower for simulations with oxide compared to the CVD low-$k$ dielectric. While the difference is small (roughly 15%) for a 5-$\mu$m metallization stack, it becomes considerable (more than 2$\times$ difference) with a thicker metallization that significantly reduces the alpha flux. Copper has a larger LET than both dielectrics, so the fail rate is lower for simulations where copper accounts for 50% of the metallization thickness. These simulations also indicate that the fail rate has a minimum between 12 and 15 $\mu$m of metallization; as the thickness increases, more alphas are stopped in the metallization. However, more alphas reach the active silicon near the Bragg peak of maximum LET, and the surviving alphas are more likely to cause upsets.

*Example 3: Mono-Energetic Proton Beam Experiments:* Fig. 6 shows the bit fail cross sections of the same SRAM induced by 30-MeV and 150-MeV protons. The proton beam measurements were performed at the Northeast Proton Therapy Center, and the simulations were done by SEMM-2. It has been pointed out that SEMM-2 calculations do not use arbitrary normalizations, and as such, the agreement between measurement and simulation is considered to be acceptable for SEU evaluation of designs.

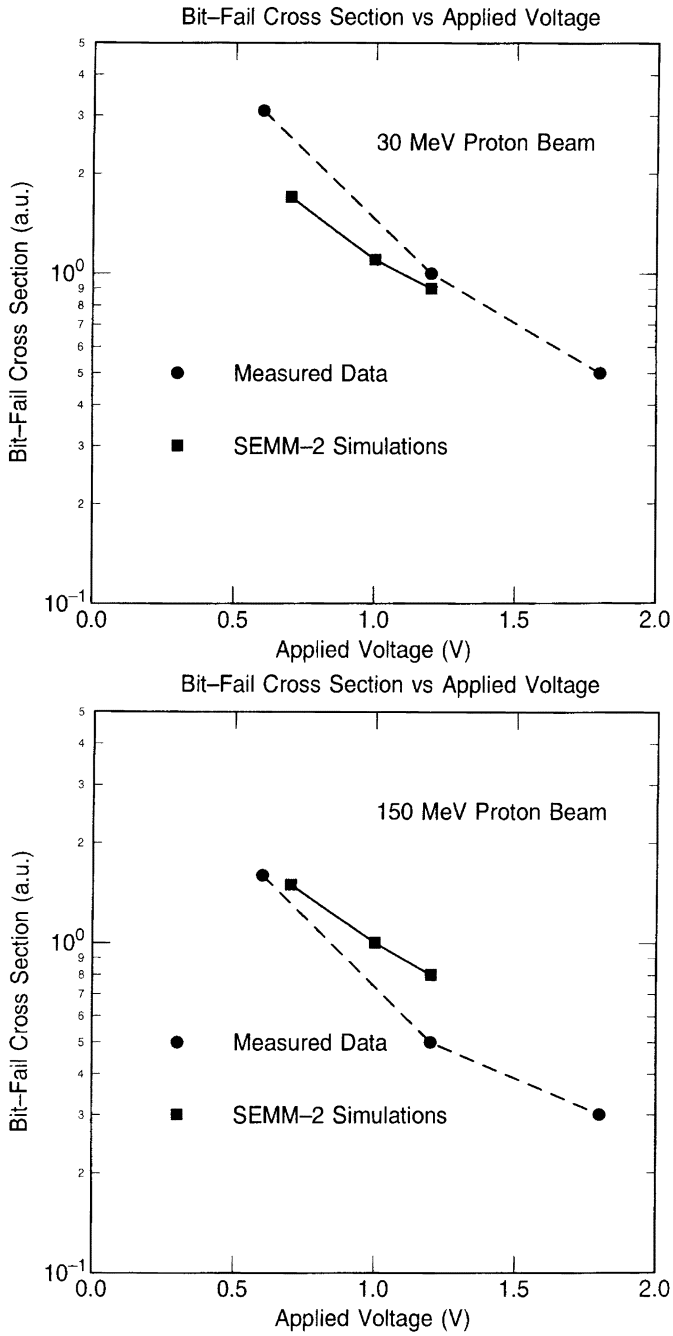


Fig. 6. SEU bit fail cross section as function of applied voltage, induced by 30-MeV and 150-MeV mono-energetic protons. The experiments are taken at the Northeast Proton Therapy Center, Boston, MA. The theoretical calculations are done with SEMM-2.

## V. Limitations of SEMM-2

In this section, we give a summary of the important sources of uncertainties of SEMM-2.

An important physics issue that is not addressed in SEMM-2 is the track structure of an incident ion. The energy deposition from the ion in a sensitive volume is computed using LET. Here one implicitly assumes that the effects of the spatial distribution of the electron-hole pairs induced by the ion strike can be ignored. In old technologies with relatively large devices, this assumption can be justified. For new devices with channel lengths below 0.1 $\mu$m, the radial extension of the electron–hole plasma

Authorized licensed use limited to: Intel Corporation via the Intel Library. Downloaded on February 27, 2009 at 14:59 from IEEE Xplore. Restrictions apply.

column induced by the heavy recoil nuclei may be a sizable portion of the device, and hence the effects of the track structure are likely to play a more significant role in SEU simulations of these technologies. Such expectations are consistent with the recent findings of Monte Carlo simulations of ion-induced secondary electrons in devices [16].

Another limitation in SEMM-2 is the treatment of the charge collection step (see Fig. 1) that eventually determines whether a particular radiation event causes fail or not. This is the most CPU consuming step. Depending on the degree of complexity of the cell being analyzed, some runs can take hours on a fast machine. Further enhancements using computationally more efficient schemes are currently considered.

One source of inaccuracy of SEMM-2 can come from the way that the code treats the metallization materials. Currently they are modeled as planar levels, whereas the true structure is far more complicated than that. Even if the LET calculations were exact, the effects of the materials' shape irregularities on the energy of an incident ion would still be difficult to estimate.

Finally, LET which plays a central role in SEMM-2 simulations, only gives the mean energy loss of an ion. Higher order effects like ion straggling at the end of the particle range are bound to play some role in SEU calculations as the devices scale down further.

## VI. Conclusion

We have developed SEMM-2, a state-of-the-art SEU simulation system, for both current and future CMOS technologies. Compared to SEMM-1, which was developed in the mid-1980s for bipolar technologies, SEMM-2 has incorporated significant enhancements that render it a robust SEU analysis tool suitable for basic research as well as for analyzing advanced CMOS product designs in the years to come.

## Acknowledgment

The authors acknowledge the support of the IBM SER team. Specifically, they have benefited from helpful discussions and productive interactions with J. Aitken, K. Bernstein, M. Gordon, D. Heidel, T. Ning, P. Oldiges, R. Puri, D. Reinhardt, K. Rodbell, and T. Zabel. The authors also thank the referees for their careful review and constructive criticisms of the paper.

## References

[1] G. R. Srinivasan, H. K. Tang, and P. C. Murley, "Parameter-free, predictive modeling of single event upsets due to protons, neutrons, and pions in terrestrial cosmic rays," *IEEE Trans. Nucl. Sci.*, vol. 41, pp. 2063–2070, Dec. 1994.

[2] G. R. Srinivasan, P. C. Murley, and H. K. Tang, "Accurate, predictive modeling of soft error rate due to cosmic rays and chip alpha radiation," in *Proc. 32nd Annu. Reliability Physics Conf.*, 1994, pp. 12–16.

[3] G. R. Srinivasan, "Modeling the cosmic-ray-induced soft-error rate in integrated circuits: An overview," *IBM J. Res. Develop.*, vol. 40, no. 1, pp. 77–89, Jan. 1996.

[4] P. C. Murley and G. R. Srinivisan, "Soft-error Monte Carlo modeling program, SEMM," *IBM J. Res. Develop.*, vol. 40, no. 1, pp. 109–118, Jan. 1996.

[5] H. H. K. Tang, "Nuclear physics of cosmic ray interaction with semiconductor materials: Particle-induced soft errors from a physicist's perspective," *IBM J. Res. Develop.*, vol. 40, no. 1, pp. 91–108, Jan. 1996.

[6] H. H. K. Tang, G. R. Srinivasan, and N. Azziz, "Cascade statistical model for nucleon-induced reactions on light nuclei in the energy range 50 MeV–1 GeV," *Phys. Rev. C42*, no. 4, pp. 1598–1622, 1990.

[7] H. H. K. Tang and K. P. Rodbell, "Single-event upsets in microelectronics: Fundamental physics and issues," *MRS Bull.*, vol. 28, pp. 111–116, 2003.

[8] R. Baumann, "Impact of single-event upsets in deep-submicron silicon technology," *MRS Bull.*, vol. 28, pp. 117–120, 2003.

[9] E. H. Cannon, D. D. Reinhardt, M. S. Gordon, and P. S. Makowenskyj, "SRAM SER in 90, 130, and 180 nm bulk and SOI technologies," in *Proc. Int. Reliability Physics Symp.*, 2004, pp. 300–304.

[10] M. S. Gordon, P. Goldhagen, K. P. Rodbell, T. H. Zabel, H. H. K. Tang, J. M. Clem, and P. Bailey, "Measurement of the flux and energy spectrum of cosmic-ray induced neutrons on the ground," *IEEE Trans. Nucl. Sci.*, vol. 51, Dec. 2004.

[11] P. Oldiges, K. Bernstein, D. Heidel, B. Klaasen, E. Cannon, R. Dennard, H. Tang, M. Ieong, and H. S. P. Wong, "Soft error rate scaling for emerging SOI technology options," in *IEEE Symp. VLSI Technology Dig. Tech. Papers*, Honolulu, HI, June 2002, pp. 46–47.

[12] J. L. Romero, H. H. K. Tang, D. J. Morrissey, M. Fauerbach, R. Pfaff, C. F. Powell, B. M. Sherrill, F. P. Brady, D. A. Cebra, J. Chance, J. C. Kinter, and J. H. Osborne, "Nucleon-induced secondaries: A review and future experimental developments," in *Amer. Inst. Physics Conf. Proc.*, vol. 392, 1997, pp. 655–658.

[13] L. L. Carter and E. D. Cashwell, "Particle-transport simulations with the Monte Carlo method," Technical Information Center Publications, Office of Public Affairs, U.S. Energy Research and Development Administration, Oak Ridge, TN, 1975.

[14] Particle Interactions With Matter—The Stopping and Range of Ions in Matter (SRIM), J. Ziegler. [Online]. Available: http://www.srim.org

[15] P. Oldiges, R. Dennard, D. Heidel, B. Klaasen, E. Assaderaghi, and M. Ieong, "Theoretical determination of the temporal and spatial structure of alph-particle induced electron-hole pair generation in silicon," *IEEE Trans. Nucl. Sci.*, vol. 47, pp. 2575–2579, Dec. 2000.

[16] R. A. Weller, private communication.

Authorized licensed use limited to: Intel Corporation via the Intel Library. Downloaded on February 27, 2009 at 14:59 from IEEE Xplore. Restrictions apply.